Frontier ocean thermal/power and solar PV systems for transformation towards net-zero communities

Liu, Zhengxuan; Zhou, Yuekuan; Yan, Jun; Tostado-Véliz, Marcos

DOI
10.1016/j.energy.2023.128362

Publication date
2023

Document Version
Final published version

Published in
Energy

Citation (APA)
Liu, Z., Zhou, Y., Yan, J., & Tostado-Véliz, M. (2023). Frontier ocean thermal/power and solar PV systems for transformation towards net-zero communities. *Energy*, *284*, Article 128362. https://doi.org/10.1016/j.energy.2023.128362

Energy 284 (2023) 128362

Contents lists available at ScienceDirect

Energy

journal homepage: www.elsevier.com/locate/energy

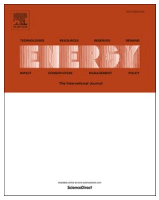

Frontier ocean thermal/power and solar PV systems for transformation towards net-zero communities

Zhengxuan Liu [a,1], Yuekuan Zhou [b,c,d,e,*], Jun Yan [f,1], Marcos Tostado-Véliz [g]

[a] Faculty of Architecture and the Built Environment, Delft University of Technology, Julianalaan 134, 2628 BL, Delft, Netherlands
[b] Sustainable Energy and Environment Thrust, Function Hub, The Hong Kong University of Science and Technology (Guangzhou), Nansha, Guangzhou, 511400, Guangdong, China
[c] HKUST Shenzhen-Hong Kong Collaborative Innovation Research Institute, Futian, Shenzhen, 518048, China
[d] Department of Mechanical and Aerospace Engineering, The Hong Kong University of Science and Technology, Clear Water Bay, Hong Kong, China
[e] Division of Emerging Interdisciplinary Areas, The Hong Kong University of Science and Technology, Clear Water Bay, Hong Kong, China
[f] Institute of Engineering Thermophysics, School of Mechanical Engineering, Shanghai Jiao Tong University, Shanghai, 200240, China
[g] Department of Electrical Engineering, University of Jaén, 23700, Linares, Spain

ARTICLE INFO

Handling Editor: X Zhao

Keywords:
Ocean thermal/power energy
Coastal oscillating water column
Solar energy
Scale sizing and energy planning
Energy management strategy
Cycling aging of battery

ABSTRACT

Ocean thermal and power energy systems are promising driving forces for seashore coastal communities to achieve net-zero energy/emission target, whereas energy planning and management on ocean thermal/power and distributed building integrated photovoltaic (BIPV) systems are critical, in terms of serving scale sizing and planning on geographical locations of district building community, and cycling aging of battery storages. However, the current literature provides insufficient studies on this topic. This study aims to address this research gap by transforming towards zero-energy coastal communities from the district level in subtropical regions, including centralised seawater-based chiller systems, distributed BIPVs and coastal oscillating water column technologies, as well as multi-directional Vehicle-to-Building energy interaction paradigms. Advanced energy management strategies were explored to enhance renewable penetration, import cost-saving, and deceleration of battery cycling aging, in response to relative renewable-to-demand difference, off-peak grid information with low price, and real-time battery cycling aging. Furthermore, in accordance with the power generation characteristic of two wave stations (i.e., Kau Yi Chau (KYC) and West Lamma Channel (WLC)) in Hong Kong, energy system planning and structural configurations of the coastal community were proposed and comparatively studied for the multi-criteria performance improvement. Research results showed that, compared to an air-cooled chiller, the water-cooled chiller with a much higher Coefficient of Performance (COP) will reduce the energy consumption of cooling systems, leading to a decrease in total electric demand from 134 to 126.5 kWh/m^2·a. The scale for the net-zero energy district community with distributed BIPVs and oscillating water column was identified as 5 high-rise office buildings, 5 high-rise hotel buildings, 150 private cars and 120 public shuttle buses. Furthermore, the geographical location planning scheme on the Case 1 (office buildings close to KYC, and hotel buildings close to WLC) was identified as the most economically and environmentally feasible scheme, whereas the Case 3 (only office buildings are planned close to all power supply with oscillating water column) showed the highest flexibility in grid electricity shifting, together with the highest value of equivalent battery relative capacity. This study demonstrates techno-economic performances and energy flexibility of frontier ocean energy technologies in a coastal community under advanced energy management strategies, together with technical guidance for serving scale sizing and planning on geographical locations. The research results highlight the prospects and promote frontier ocean energy techniques in subtropical coastal regions.

* Corresponding author. Sustainable Energy and Environment Thrust, Function Hub, The Hong Kong University of Science and Technology (Guangzhou), Nansha, Guangzhou, 511400, Guangdong, China.
E-mail addresses: yuekuanzhou@ust.hk, yuekuan.zhou@outlook.com (Y. Zhou).
[1] Zhengxuan Liu and Jun Yan contributed equally to the work.

https://doi.org/10.1016/j.energy.2023.128362
Received 21 May 2023; Received in revised form 24 June 2023; Accepted 7 July 2023
Available online 13 July 2023

1. Introduction and background

To address the conflicting contradiction between intensified energy crisis and daily increased energy demands, mitigate global warming and climate change, continuous efforts have been made to search for new power production resources [1–3]. Electrification, hydrogenation [4] and cross-regional energy sharing [5] with e-mobility integration have attracted researchers' interests, particularly with the call for carbon neutrality by 2060. Pathways for carbon neutrality in different regions are diverse [6], depending on local climate conditions, regional energy consumption profiles, renewable energy supplies and other factors [7,8]. Ocean energy systems have gained widespread interest in coastal communities due to their multi-diversified energy forms (such as ocean thermal and electrical energy), advanced energy conversions (cooling power production via water-cooled chiller, and power generator via wave energy converter, tidal stream generator, and Organic Rankine Cycle (ORC)), abundance in power production, and stability in spatio-temporal distributions [9,10]. Unlike the sole availability of solar energy during sunny daytime, the ocean energy is more spatially even and less dependent on the calendar date [11,12]. Meanwhile, compared to low air density for wind power generation, ocean power energy from wave energy converters and tidal stream generators is more promising due to larger water density [13].

Both ocean thermal and power systems are included for different energy forms. Due to stable seawater temperature, seawater cooled chiller is full of prospects for cooling applications due to the relatively high coefficient of performance (COP). The dynamic performance comparison between air cooling chiller, direct and indirect seawater cooling systems showed that, compared to the air-cooled chiller system, the indirect seawater chiller can improve the COP due to the low seawater temperature [14]. Meanwhile, compared to the direct seawater chiller, the indirect seawater chiller will reduce initial and maintenance costs. However, due to the corrosion issue on the piping system, the seawater chiller system needs to be well designed and requires special maintenance. In addition to thermal systems, ocean power energy systems have also been popular due to considerable power generation potentials for wave energy, tidal energy, solar and wind energy on the sea [15]. Compared to the frequent change of tidal range and water head, and in-depth installation of tidal generator, wave energy systems mainly float on the sea with large power generation potentials. In academia, researchers mainly focused on experimental performance analysis [16], modelling development [17], parametric analysis and optimisation [18]. The design guidance on OWC was provided for high-efficient utilisation of mechanical ocean energy [17]. The systematic review was provided on fixed and floating hollow structure-based wave energy converters [18], in terms of theoretical, numerical and experimental modelling techniques. Results showed that peak and average efficiencies are around 80% and above 70%, respectively. For random waves, an experimental study was conducted on oscillating water column [16]. The conversion of air kinetic into electric energy can bring additional benefits and prospects for ocean energy application. However, there are limited studies on applications of ocean thermal and power systems in a coastal residential community, especially considering the spatiotemporal difference in power supplies and demand diversity of different building types.

Energy system planning and scale sizing are critical for the transition towards sustainability of district building communities [19]. A comprehensive review on optimal design approaches was provided [20]. Upadhyay and Sharma [21] indicated that, analytical techniques were widely used for system sizing, whereas artificial intelligence methods sometimes become ineffective. Liu et al. [22] emphasized the importance of hybrid renewable systems and called for sophisticated models to account for the distinctive characteristics and applicability of isolated areas. Additionally, energy storage systems have been widely applied to address the intermittency and instability of renewable energy. In term of the response time, Zhou et al. [23] concluded that battery storage systems are superior in responding to long-period power fluctuations. Depending on the dynamic charging/discharging power, cycling aging of battery system will significantly affect the techno-economic feasibility. Zhou et al. [24] characterized the real-time cycling aging of hybrid building and vehicle batteries in a neighbourhood-based district energy community. The proposed modelling approach and controls can provide paradigmatic guidance to system designers, operators, and stakeholders. The lifecycle-based techno-economic feasibility analysis

Nomenclature

Symbols

C	cost
E	energy
G	renewable generation [kWh]
H	wave height
P	power
l	length
T	temperature (°C)
k	wave number

Greek

α	absorbance
τ	time-duration step [h]
w	width
λ	distance
ρ	density

Subscripts

AC	air handling unit cooling
DHW	domestic hot water
exp	export to the electric grid
e	electricity
REe	renewable energy
imp	import from the electric grid
light	lighting
short	shortage
surp	surplus
SC	space cooling

Abbreviations

AHU	air handling unit
ACST	air handling unit cooling storage tank
BIPV	building integrated photovoltaic
COP	Coefficient of Performance
ECE	equivalent CO_2 emission
GSR	grid-shifted ratio
IC	import cost
ORC	Organic Rankine Cycle
RC	relative capacity
REe	renewable electricity
RSR	renewable shifted ratio
RPR	renewable penetration ratio
SCR	self-consumption ratio
SCST	space cooling storage tank

Table 1
Overview of energy management strategies for renewable supported buildings and transportation systems.

Studies	Systems	Energy management strategies	Assessment criteria	Conclusions
Zhou and Cao [27]	High-rise building integrated with vehicle fleets	1) renewable-to-demand and grid-responsive control; 2) off-peak grid charging control	Cost, CO_2 emission and energy flexibility	The proposed grid-responsive control can improve the energy flexibility.
Zhou et al. [24]	A neighbourhood-based energy sharing system	Protective control strategy	Import cost, equivalent CO_2 emission and equivalent relative capacity	Battery relative capacity can be improved from 0.743 to 0.921.
Zhou and Cao [25]	A neighbourhood -based energy sharing system	1) renewable-to-demand strategy; 2) off-peak grid-responsive control; 3) battery-protective strategy	Net present value and discounted payback time	Battery-protective strategy and economic incentive policy are necessary.
Zhou and Cao [32]	Wind turbine supported residential building	REe-to-demand control & battery-to-demand control	Energy flexibility	REe-to-demand control can shift more forced electricity and delayed electricity.
Yan et al. [33]	Distributed battery storage based smart microgrid	Smart community microgrid (SCMG) based swappable battery storage	Renewable penetration and economic cost	The proposed strategy can realise more than 60% of renewable penetration, and reduced economic cost.
Pascual et al. [28]	Renewable-based residential microgrid	SoC based control	Power peaks and fluctuations	Stable grid power profile can be realised for a given battery via the proposed control strategy.
Zhou et al. [34]	A neighbourhood-based energy sharing system	1) renewable-to-demand strategy; 2) off-peak grid-responsive control; 3) battery-protective control	Net present value and discounted payback time	Energy paradigm transition can improve net present value and reduced net direct energy consumption.
Liu et al. [35]	Commercial buildings integrated with PV and advanced energy storage	Time-of-use energy management strategy	Cost, CO_2 emission, load coverage	The proposed strategy can achieve a 95.14% reduction in carbon emissions compared to conventional grid supply.

[25] indicated that the consideration of cycling aging will lead to economic infeasibility for expanded battery storage, and necessitating advanced energy control strategies for battery protection. It is noteworthy that, system scale sizing and planning are mainly on distributed PV-battery systems, whereas the serving scale sizing for ocean power energy systems of district building communities is quite rare. Furthermore, geographical location of district building communities along the coastal line for ocean energy utilisation are quite necessary to be explored for energy planning strategies.

Energy management strategies on distributed renewable systems and ocean energy have attracted researchers' interests in district communities [26], to improve techno-economic-environment performance. Table 1 lists an overview of energy management strategies for renewable-supported buildings and transportation systems. Zhou and Cao [27] comparatively explored different energy control strategies for an office building integrated with vehicles. Results showed that, the proposed strategy can effectively shift off-peak power, whereas energy congestions between renewable and off-peak power energy needs to be well addressed via the static battery storage design. From the lifecycle-based perspective, Zhou and Cao [25] developed battery-protective strategy, and provided in-depth analysis on grid feed-in tariff. In response to intermittent renewable energy, the battery-protective strategy is quite necessary for economic feasibility assessment, especially for the expensive cost of battery systems. Furthermore, from the perspective of power grid, Pascual et al. [28] developed a state of charge based control, to realise stable grid power profile. The proposed strategy can smooth power peaks and fluctuations for intermittent renewable integrations. It is noteworthy that energy management strategies are mainly on distributed PVs and wind turbines, whereas effective solutions for ocean energy management for district community applications are quite rare. Furthermore, decentralized load control [29], climate-based energy consumption [30,31] are also explored as effective solutions.

Scientific knowledge gaps that exist in the field of integrated ocean energy systems for coastal residential communities are summarized below. Firstly, due to the relatively high specific density, the conversion of air kinetic and gravitational potential energy from ocean into electric energy is full of promising prospects. However, there are limited studies on applications of integrated ocean thermal and power systems in coastal residential communities, especially for the spatiotemporal difference in power supplies and demand diversity of different building types. Secondly, the serving scale sizing of district communities with integrated ocean energy technologies has not been quantified yet. Planning strategies on geographical location of district building community along the coastal line for ocean energy utilisation are quite necessary to be explored. Thirdly, energy management strategies are mainly on distributed PVs and wind turbines, whereas effective solutions for ocean energy management in district community applications are quite rare.

Research contributions and originalities of this study are summarized as follows:

1) an integrated platform is developed for energy planning, design, operation, to promote transformation of net-zero energy coastal communities.
2) energy synergies are explored and multi-criteria performance potentials are quantitatively analysed among centralised seawater-based chiller systems, distributed BIPVs and coastal oscillating water column, and smart Vehicle-to-Building interactions.
3) energy system planning and structural configurations of the coastal community are proposed, to provide technical guidelines on system scale sizing, energy planning on geographical locations in coastal district communities.

Section 2 introduces the integrated system design and local grid information. Section 3 shows energy management strategies and multi-

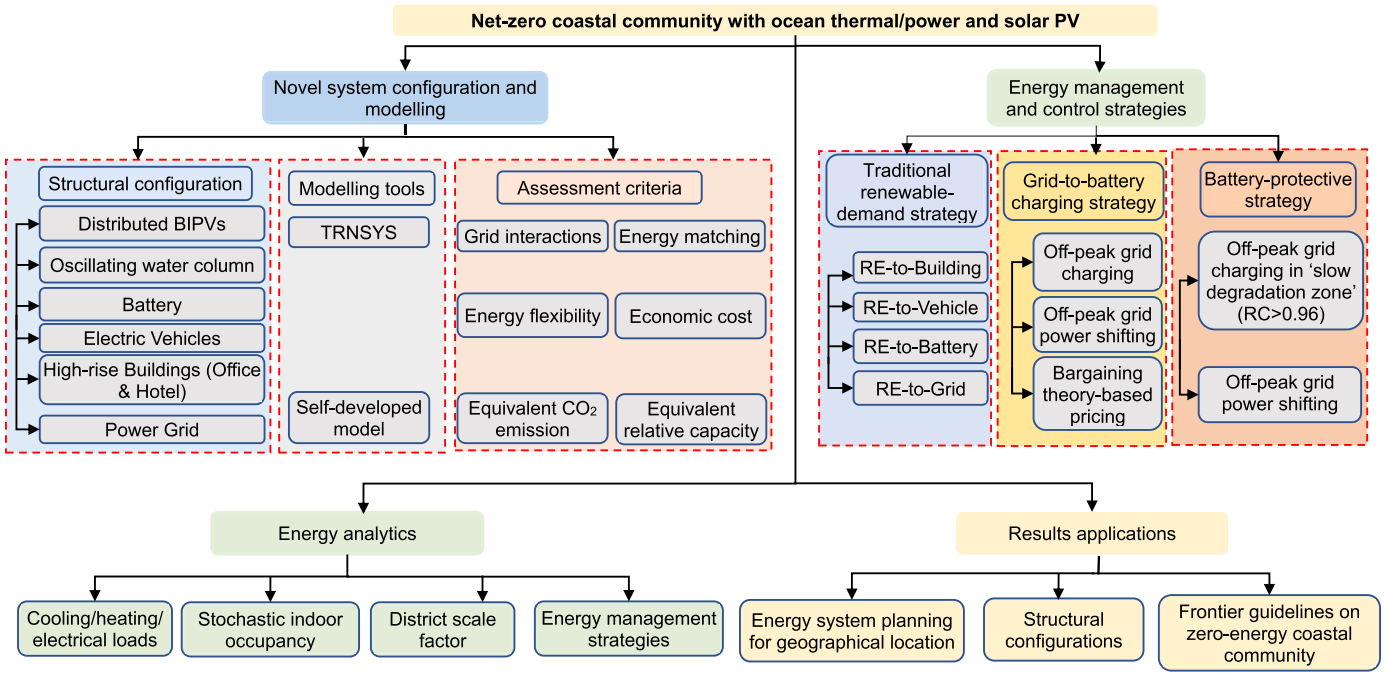

Fig. 1. A holistic overview of the research framework.

criteria. Building energy analysis is presented in Section 4. Results, discussion and conclusions are in Section 5 and 6, respectively.

2. Research framework

Fig. 1 illustrates the research framework of this study, including novel system configuration and modelling, energy management and control strategies, energy analytics, and results applications. Specifically, the system configuration involves distributed BIPVs, oscillating water column, battery, Electric Vehicles, high-rise buildings (Office & Hotel) and power grid. The multi-energy system is developed TRNSYS and evaluated by multiple assessment criteria, including grid interactions, energy matching, energy flexibility, economic cost, equivalent CO_2 emission, and equivalent relative capacity of batteries. Afterwards, different energy management and control strategies (i.e., traditional renewable-demand strategy, grid-to-battery charging strategy and battery-protective strategy) are applied and compared, followed by energy analytics, including cooling/heating/electrical loads, stochastic indoor occupancy, district scale factor and energy management strategies. Lastly, research results applications are provided in energy system planning for geographical location, structural configurations and frontier guidelines on zero-energy coastal communities.

3. Description on multi-energy systems in a coastal community

3.1. System configuration

Fig. 2 demonstrates the schematic diagram of the district community designed in this study, which utilizes both oscillating water column and BIPVs as clear energy supply. The system scale is case-dependent, and the district scale factor is used to represent the scale of the coastal community. Specifically, the district community includes a 30-floor office, a 30-floor hotel, 30 EVs and 24 public shuttle buses, when the district scale factor is 1. The district community includes n 30-floor office, n 30-floor hotel, 30xn EVs and 24xn public shuttle buses, when the district scale factor is n.

3.2. HVAC, energy storage and vehicle systems

Table 2 shows the detailed parameters of air-cooled and water-cooled chillers. Fig. 3 illustrates the systematic configuration of cooling systems, including air-handling unit (AHU) cooling and space cooling with chilled water temperature at 7 and 15 °C, respectively. The AHU cooling aims to dehumidify and cool down supply air, and the space cooling is intended to cool down the supply air.

Thermal and electric storages are shown in Table 3, and vehicle batteries are shown in Table 4, with battery capacity for electric vehicle at 58 kWh (Opel Ampera-e) and 200 kWh [36], respectively. It is noteworthy that, the benchmark case includes a 30-floor office, a 30-floor hotel, 30 private cars and 24 public shuttle buses. The expansion of the district community scale is expressed by the district scale factor, with the consideration on stochastic indoor occupancy.

3.3. Distributed solar energy system and oscillating water column

In this study, both distributed solar energy system and oscillating water column are applied for cleaner power production. Dynamic depreciation rate of BIPVs is 0.5%/year [37].

In order to calculate the power contained in ocean waves, mathematical sine function was adopted to describe the shape of a typical wave. Depending on the types of water waves in different depths, the wavelength λ can be calculated by following equations:

$$\lambda = \begin{cases} \dfrac{gT^2}{2\pi} & deep\ wave \\ \sqrt{gD}T & shallow\ waves \end{cases} \quad (1)$$

where T is the wave period. D is the water depth, and g is the gravity (9.81 m/s^2). π is circular constant at 3.1415926 ….

The periodic energy E_t and the average power P_t can be calculated as follows [38]:

$$E_t = \frac{32}{81\pi A_c^2}\rho T w^3 H^3 \lambda^3 \sin^3\left(\frac{kl}{2}\right) \quad (2)$$

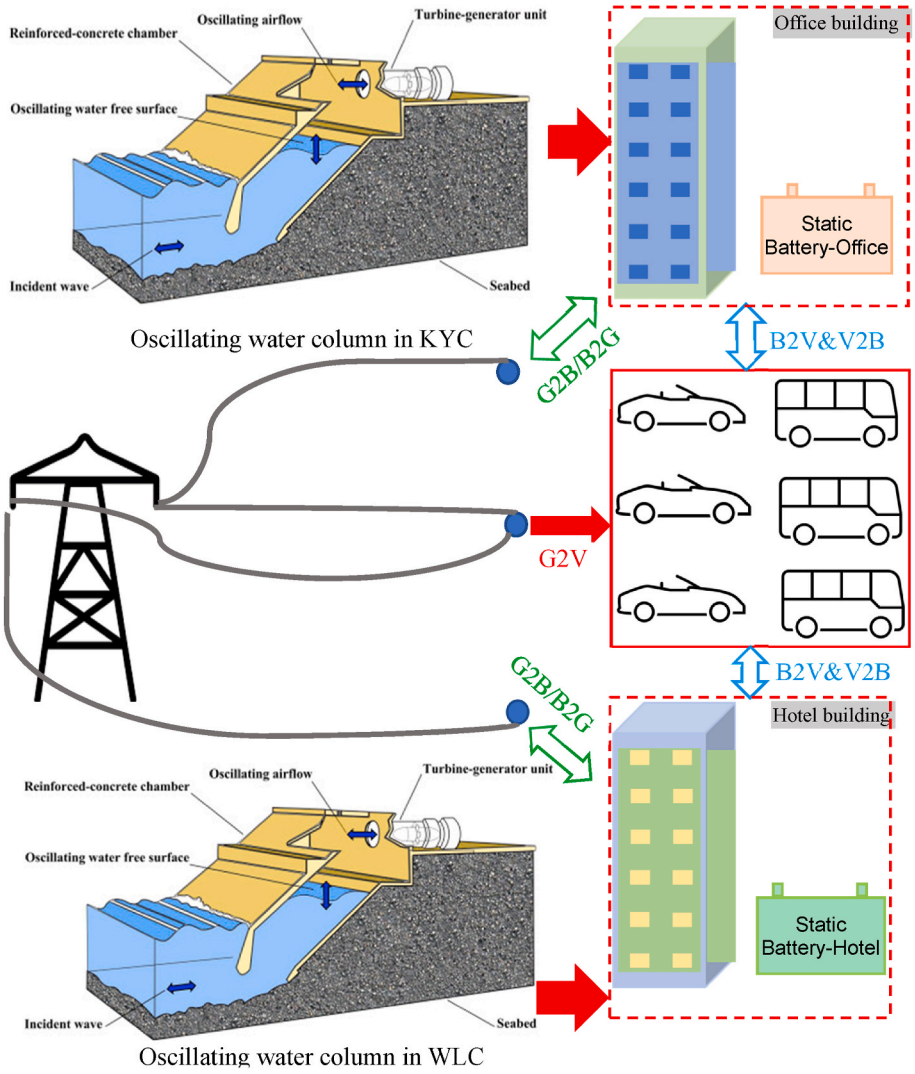

Fig. 2. Schematic diagram for oscillating water column and BIPVs integrated district coastal community (benchmark case).

$$P_t = \frac{32\rho}{81\pi A_c^2 T^2} w^3 H^3 \lambda^3 \, sin^3\left(\frac{\pi l}{\lambda}\right) \tag{3}$$

$$k = \frac{2\pi}{\lambda} \tag{4}$$

where A_c is the area of the turbine cross section. The wave height H (difference in height between peaks and troughs), the wave length λ (the distance between successive peaks (or troughs) of the wave), and the wave period T (seconds taken for successive peaks (or troughs) to pass a given fixed point). ρ is the air density. w and l is the width and length of the chamber. k is the wave number.

4. Energy management system, control strategies and system assessment criteria

4.1. Energy management and control strategies

Fig. 4 demonstrates power flow chart of the integrated net-zero coastal community with ocean thermal/power and solar PV systems. There are three strategies for different purposes, i.e., traditional renewable-demand strategy (Control Strategy 1, Reference case), grid-to-battery charging strategy (Control Strategy 2, operating cost saving) and battery-protective strategy (Control Strategy 3, battery relative capacity improvement). In respect to traditional renewable-demand strategy (Control Strategy 1) in Fig. 4(a), after covering the energy demands, the surplus renewable energy flows to charge vehicle and static batteries, before being exported to the grid. Demand shortage will be covered by static battery, vehicle battery, and then by power grid. Considering the difference in peak and off-peak grid electricity prices (i.e., 0.9 HK$/kWh from 9:00 a.m. to 21:00 p.m. and 1.1 HK$/kWh from 21:00 p.m. to 9:00 a.m.), the grid-to-battery charging strategy (Control Strategy 2) in Fig. 4(b) is developed to demonstrate the off-peak grid charging for power shifting. The ultimate object is to save operational costs by shifting the low-price grid electricity to the high-price price period. Furthermore, considering the battery cycling ageing during the low-price grid electricity shifting period, the battery-protective strategy (Control Strategy 3) in Fig. 4(c) restrains the off-peak grid charging within the RC threshold higher than 0.96 ('slow degradation zone'). This is to guarantee the economic feasibility by reaching the trade-off between battery cycling ageing cost and cost saving from the low-price grid electricity shifting.

4.2. Multi-criteria for coastal community assessment

4.2.1. Grid interactions

The annual imported/exported energy, as shown in Equations (5) and (6), were adopted for the energy performance assessment.

Table 2
Specifications on air-cooled and water-cooled chillers.

Buildings	Air-cooled chillers				Water-cooled chillers			
	AHU chiller		Space cooling chiller		AHU chiller		Space cooling chiller	
	Office	Hotel	Office	Hotel	Office	Hotel	Office	Hotel
Products	Carrier 30RB302 (30RB 162–802)	CGAD090	Carrier 30RB522 (30RB 162–802)	Carrier 30RB302 (30RB 162–802)	Daikin WGZ200 (WGZ-D_02.16.2015_DA, 200 Tons)	Daikin WGZ30 (WGZ-D_02.16.2015_DA, 30 Tons)	Carrier30XW802 (30XW-30XWH)	Daikin WGZ200
Rated capacity (kW)	293	93.9	506	293	293	93.9	506	293
Nominal COP	2.8	3.2	2.6	2.8	4.7	4.2	5.5	4.7
Set-point temperature	7 °C		15 °C		7 °C		15 °C	

$$E_{imp,a} = \int_{ti}^{te} P_{imp}(t)\,dt \Big/ A \tag{5}$$

$$E_{exp,a} = \int_{ti}^{te} P_{exp}(t)\,dt \Big/ A \tag{6}$$

where the $P_{imp}(t)$ and the $P_{exp}(t)$ are the instantaneous electric power imported from and exported to the electric grid, [kW], respectively. The $E_{imp,a}$ and the $E_{exp,a}$ indicate the annual electricity imported from and exported to the grid, respectively. 'dt' is the time step during the whole simulation. A is the area of the building. t_i and t_e refer to the starting and ending time of the simulation analysis.

4.2.2. Annual matching capability

The self-consumption ratio (SCR) and the renewable penetration ratio (RPR) are adopted to quantitatively investigate the annual matching capability of the electric energy, as shown in Equations (7) and (8).

$$SCR = \frac{\int_{t_i}^{t_e} Min[P_{REe}(t); L(t)]dt}{\int_{t_i}^{t_e} L(t)dt} \quad 0 \le SCR \le 1 \tag{7}$$

$$RPR = \frac{\int_{t_i}^{t_e} Min[P_{REe}(t); L(t)]dt}{\int_{t_i}^{t_e} P_{REe}(t)dt} \quad 0 \le RPR \le 1 \tag{8}$$

where the $P_{REe}(t)$ and $L(t)$ refer to renewable power and demand at time t.

4.2.3. Energy flexibility

Renewable shifted ratio (RSR) and grid-shifted ratio (GSR) are calculated to quantify the energy flexibility.

$$E_{off-peak,REe} = \int_0^{t_{off-peak}} \left[P_{toSB,REe}(t) + P_{toEV,REe}(t) + P_{toShutBus,REe}(t)\right] dt \tag{9}$$

$$E_{surp,REe} = \int_0^{t_{end}} P_{surp,REe}(t)dt \tag{10}$$

$$RSR = \frac{E_{off-peak,REe}}{E_{surp,REe}} \tag{11}$$

$$E_{off-peak,grid} = \int_0^{t_{off-peak}} \left[P_{toSB,grid}(t) + P_{toEV,grid}(t) + P_{toShutBus,grid}(t)\right] dt \tag{12}$$

$$E_{imp} = \int_0^{t_{end}} P_{imp}(t)dt \tag{13}$$

$$GSR = \frac{E_{off-peak,grid}}{E_{imp}} \tag{14}$$

where $E_{off\text{-}peak,REe}$ refers to renewable energy during the off-peak period. $E_{surp,Re}$ refers to the surplus renewable energy. $E_{off\text{-}peak,grid}$ refers to grid electricity during the off-peak period. E_{imp} refers to the grid import electricity. $P_{toSB,REe}(t)$, $P_{toEV,REe}(t)$ and $P_{toShutBus,REe}(t)$ refer to renewable power charged into static battery, EV and shuttle buses at time t. $P_{surp,REe}(t)$ refers to surplus renewable power. $P_{toSB,grid}(t)$, $P_{toEV,grid}(t)$ and $P_{toShutBus,grid}(t)$ refer to grid power charged into static battery, EV battery and Shuttle bus battery. $P_{imp}(t)$ refers to grid import power.

4.2.4. Economic performance

Operational costs are calculated as follows:

$$IC_{office} = \int_{ti}^{te} P_{imp,office}(t) \cdot C_{eg,imp}(t)dt \tag{15}$$

$$IC_{hotel} = \int_{ti}^{te} P_{imp,hotel}(t) \cdot C_{eg,imp}(t)dt \tag{16}$$

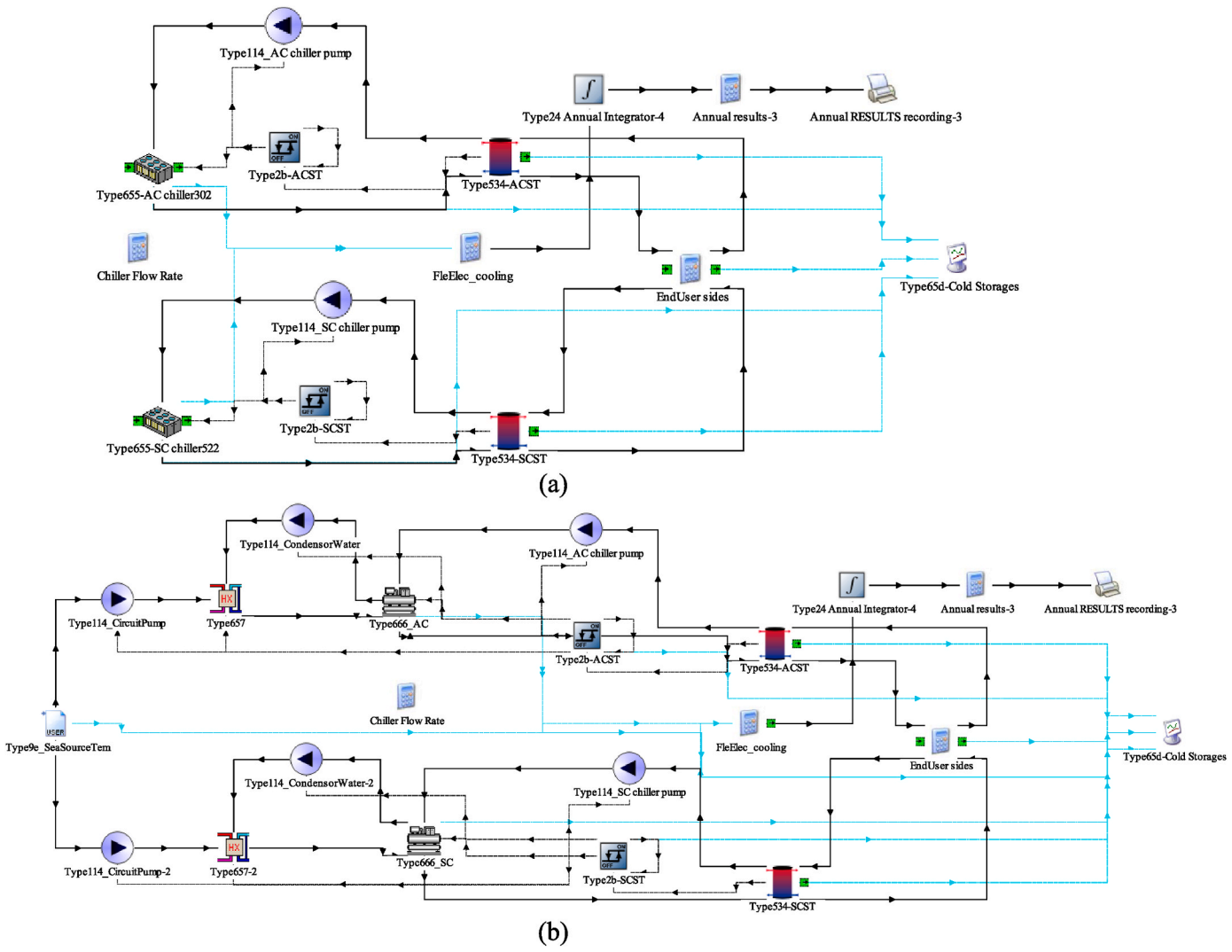

Fig. 3. Systematic configuration of cooling systems in TRNSYS 18: (a) air-cooled chiller; (b) water-cooled chiller.

Table 3
Thermal and electric storages.

	AHU/Space cooling tank	DHW tank (office/hotel)	Battery
Size (volume)	25/15 m^3	0.45/4.5 m^3	300 kWh
Heat loss coefficient	0.3 W/(m^2·K)		

Table 4
Battery-based electric vehicles for the benchmark case.

	Battery capacity (kWh)	Travelling distance (km/d)	Electricity consumption (kWh/km)	Numbers
EV-1	58	45.5	0.15 (NISSAN LEAF)	10
EV-2		35.5		10
EV-3		25.5		10
Mini-bus in each group	200	31.2	1.2 (Land Transport Guru)	24

$$IC_{Vehicles} = \int_{ti}^{te} P_{imp,vehicles}(t) \cdot C_{eg,imp}(t) dt \quad (17)$$

$$IC = IC_{office} + IC_{hotel} + IC_{Vehicles} \quad (18)$$

where IC_i, $IC_{Vehicles}$ and IC refer to import cost of the ith building, vehicles and the entire system, respectively. $P_{imp,i}$ (t) refers to the grid import power of the ith building at time t. $C_{eg,imp}(t)$ refers to grid electricity price of power grid.

4.2.5. Annual net equivalent CO_2 emissions

Annual net equivalent CO_2 emissions are calculated as follows:

$$ECE_{office} = \int_{ti}^{te} \left[P_{imp,office}(t) \cdot CEF_{eg}(t) — P_{exp,office}(t) \cdot CEF_{eg}(t) \right] dt \quad (19)$$

$$ECE_{hotel} = \int_{ti}^{te} \left[P_{imp,hotel}(t) \cdot CEF_{eg}(t) — P_{exp,hotel}(t) \cdot CEF_{eg}(t) \right] dt \quad (20)$$

$$ECE_{Vehicles} = \int_{ti}^{te} \left[P_{imp,vehicles}(t) \cdot CEF_{eg}(t) \right] dt \quad (21)$$

$$ECE = ECE_{office} + ECE_{hotel} + ECE_{Vehicles} \quad (22)$$

where ECE_i, $ECE_{Vehicles}$ and ECE refer to equivalent CO_2 emission of the

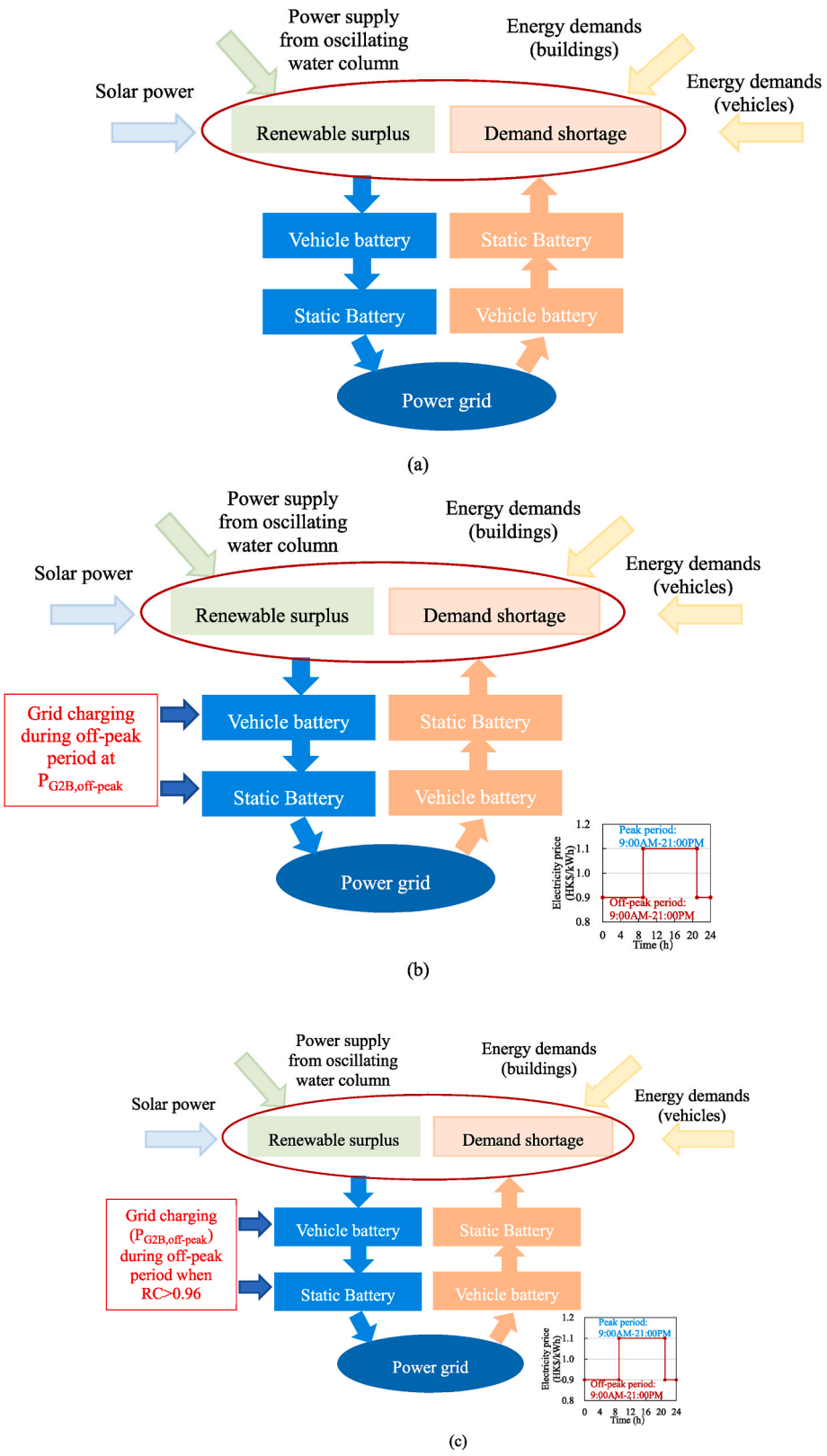

Fig. 4. Power flow chart of (a) traditional renewable-demand strategy (Control Strategy 1); (b) grid-to-battery charging strategy (Control Strategy 2); (c) battery-protective strategy (Control Strategy 3).

ith building, vehicles and the entire system, respectively. CEF_{eg} is equivalent CO_2 emission factor at 0.7 kg $CO_{2,eq}$/kWh_{end}. $P_{exp,i}$ (t) refers to the grid export power of the ith building at time t. Other variables are defined above.

4.2.6. *Equivalent relative capacity*

Considering dynamic aging during charging/discharging cycles, the equivalent relative capacity ($RC_{total,end}$) can be calculated by Equation (23) [24]:

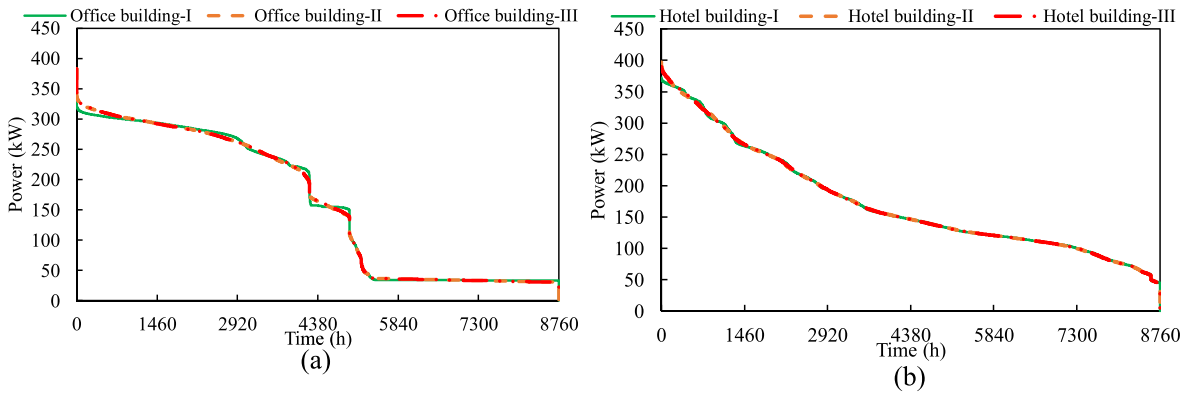

Fig. 5. Duration curve of total electrical demands for high-rise buildings in coastal residential community: (a) office buildings; (b) hotel buildings.

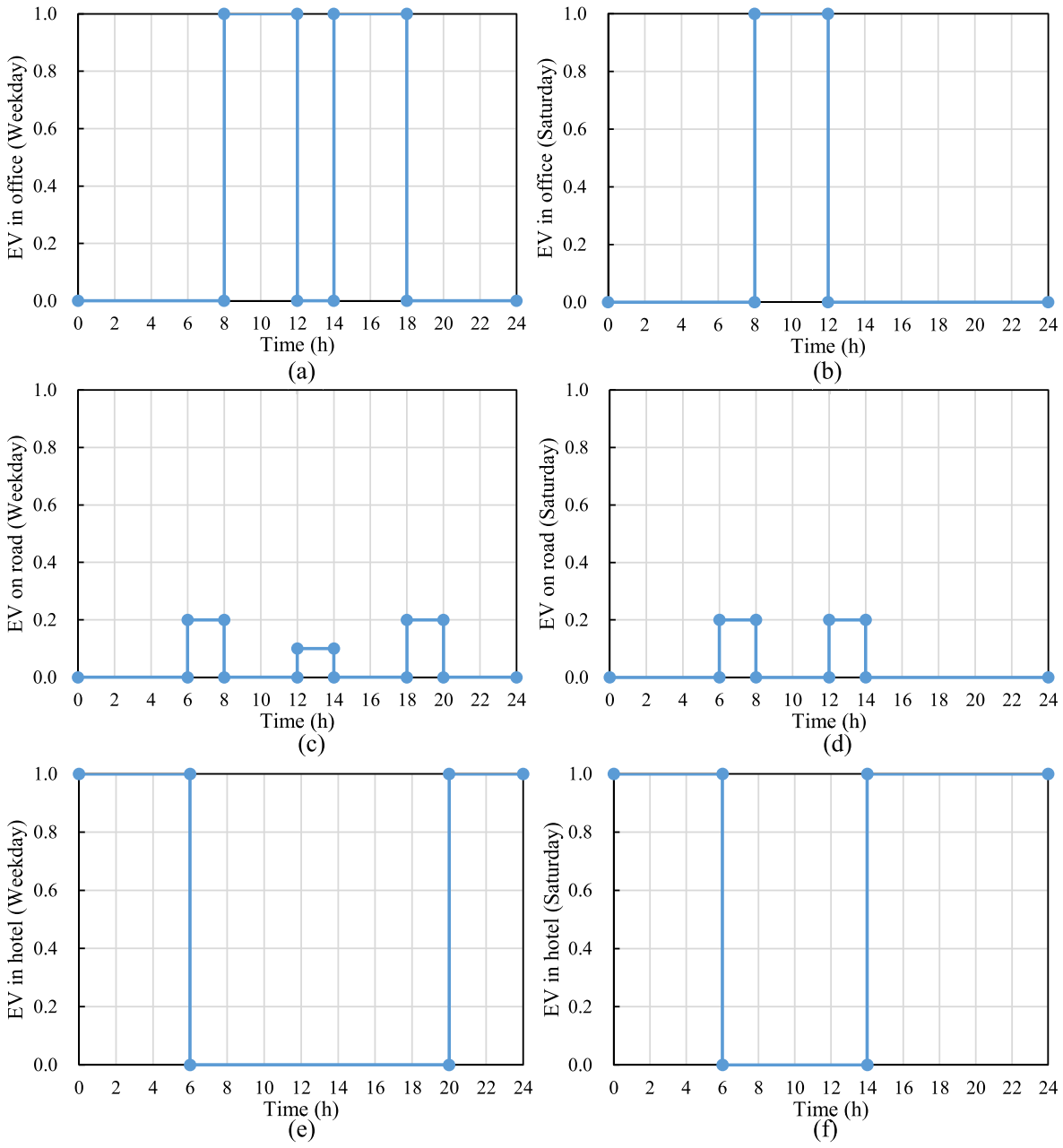

Fig. 6. EVs schedules: (a) EV in office (weekday); (b) EV in office (Saturday); (a) EV on road (weekday); (b) EV on road (Saturday); (a) EV in hotel (weekday); (b) EV in hotel (Saturday).

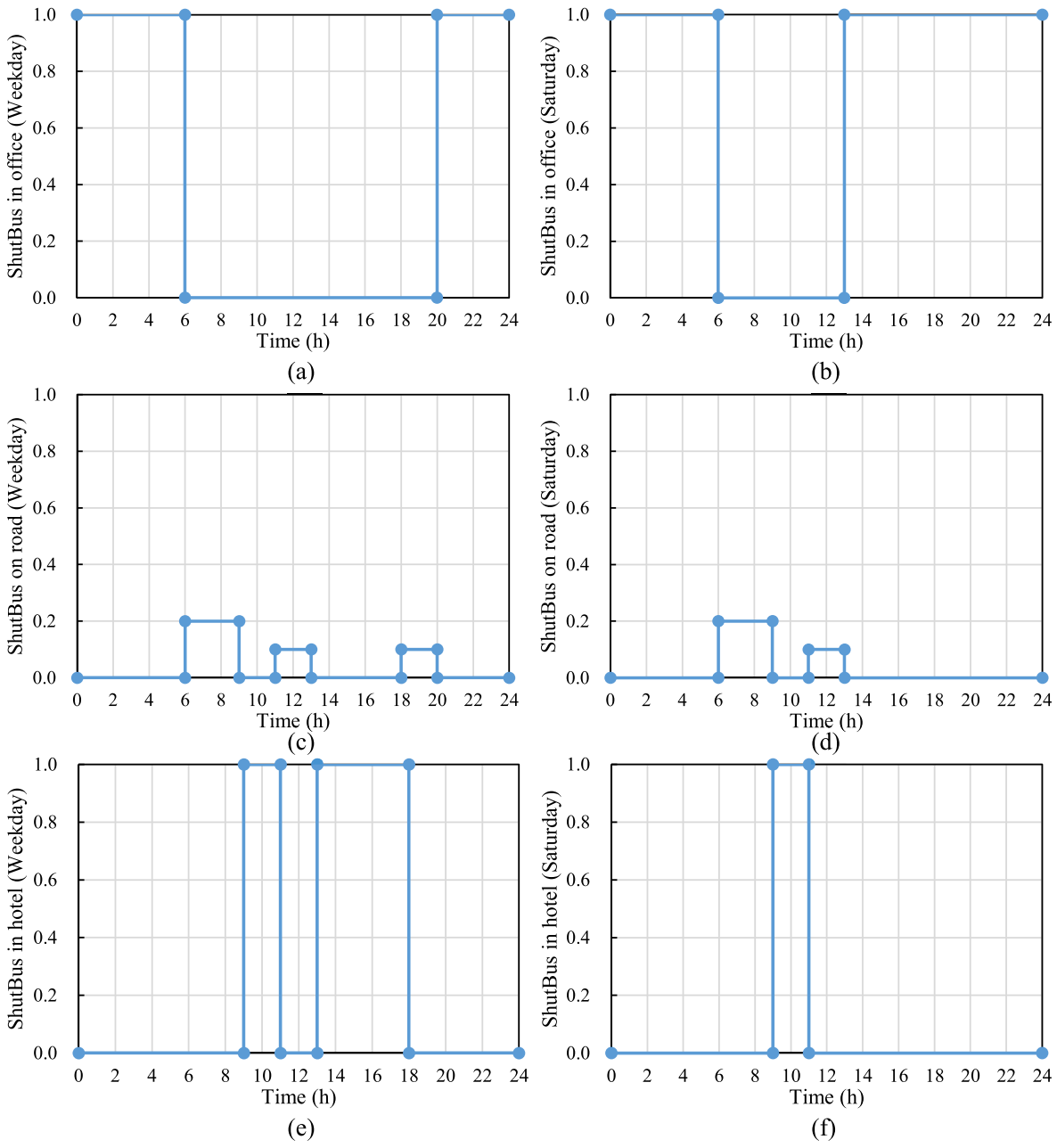

Fig. 7. Shuttle Bus schedules: (a) Shuttle Bus in office (weekday); (b) Shuttle Bus in office (Saturday); (a) Shuttle Bus on road (weekday); (b) Shuttle Bus on road (Saturday); (a) Shuttle Bus in hotel (weekday); (b) Shuttle Bus in hotel (Saturday).

$$RC_{total,end} = \sum_{i=1}^{8} \frac{Cap_{i,ini}}{Cap_{total,ini}} \times RC_{i,end} \tag{23}$$

where $Cap_{i,ini}$ and $Cap_{total,ini}$ refer to initial capacity of the ith battery and total battery groups. $RC_{i,end}$ refers to the relative capacity of the ith battery at the end.

5. Energy demands of the coastal residential community, distributed renewable energy and ocean energy generations

5.1. Stochastic indoor occupancy-based energy consumptions

Considering the diversity of indoor occupancy, the impact of stochastic indoor occupancy on heat gain was considered, with a simple assumption through a stochastic factor ($f_{stochastic}$). This is to differtiate the difference in building energy consumption of different buildings in the same category (like office and hotel).

Fig. 5 shows the duration curves of office and hotel buildings with the consideration of stochastic indoor occupancy. As shown in Fig. 5, the peak powers of office buildings are 361.8, 382.7 and 382.8 kW, respectively. Meanwhile, the peak powers of hotel buildings are 372.1, 397.1 and 389.8 kW, respectively.

$$\text{Gain}_{\text{occupant}} = f_{stochastic} \text{ xSchedule}_{\text{Occupant}} \text{xGain}_{\text{Occupant,max}} \tag{24}$$

$$\text{Gain}_{\text{equipment}} = f_{stochastic} \text{ xSchedule}_{\text{equipment}} \text{xGain}_{\text{equipment,max}} \tag{25}$$

$$\text{Gain}_{\text{light}} = f_{stochastic} \text{ x Occupant}_{\text{light}} \text{ x Gain}_{\text{light,max}} \tag{26}$$

$f_{stochastic}$ refers to the stochastic factor, ranging from 0 to 1. Schedule_i and Gain_i refer to the schedule and heat gain of the ith item.

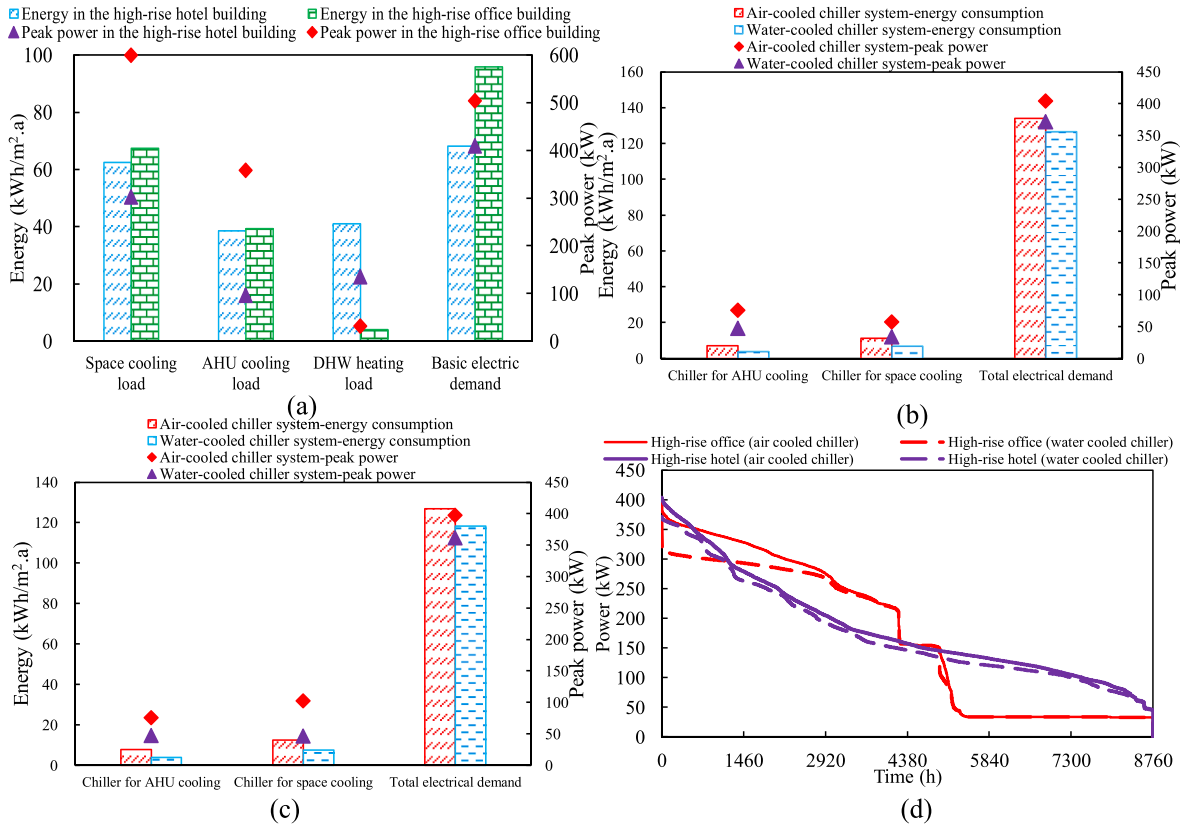

Fig. 8. Building loads and energy consumptions: (a) energy loads in office and hotel; (b) energy consumptions for air-cooled and seawater cooled chiller systems in the hotel; (c) energy consumptions for air-cooled and seawater cooled chiller systems in the office; (d) duration curves.

5.2. Deterministic schedules for electric vehicles

In terms of EV schedules, deterministic schedules are adopted for EV in office, EV on road and EV in hotel during weekday and Saturday, as shown in Figs. 6 and 7. The EV schedule refers to the proportion of EV numbers within the group. For instance, 0.2 means 20% of EVs are driving on the road. Note that, EVs are in hotel and Shuttle Buses are in office at Sunday. There three EVs groups and the number of EVs is 10 for each group. There are three Shuttle Buses groups with number of Shuttle Buses at 8 for each group. Slight differences are between each group and the schedule as shown in Figs. 6 and 7.

5.3. Cooling/heating/electrical loads and energy consumptions

In this section, cooling/heating/electrical loads and energy consumptions have been demonstrated. The impact of the ocean-water cooled chiller on the energy consumption has been studied through the comparison with the traditional air-cooled chiller system. The energy loads are preliminary for system design, and the quantified energy consumptions are the preparation for renewable system and energy management.

As shown in Fig. 8(a), compared to hotel building with the space cooling load at 62.4 kWh/m^2·a and the DHW heating load at 41 kWh/m^2·a, the office building shows a higher space cooling load at 67.5 kWh/m^2·a and a lower DHW heating load at 4.0 kWh/m^2·a. The high space cooling load in the office is due to the intensified indoor occupancy, while the high DHW heating load is mainly due to the daily shower. Furthermore, the basic electric demand in the office is 95.9 kWh/m^2·a, much higher than that in the hotel at 68.1 kWh/m^2·a. From the perspective of peak power, except for DHW heating, the office building shows much higher peak power than that in the hotel, like space cooling load, AHU cooling load and basic electric demand.

Based on the cooling loads, comparative analysis between air-cooled and water-cooled chiller systems indicates that, the seawater-based chiller system is more energy saving than air-cooled chiller system. For instance, in the hotel building as shown in Fig. 8(b), compared to air-cooled chiller system, the water-cooled chiller system will reduce the energy consumption of AHU cooling system from 6.9 to 3.8 kWh/m^2·a, the space cooling system from 11.3 to 6.9 kWh/m^2·a, and total electric demand from 134 to 126.5 kWh/m^2·a. Similar tendency can be noticed in the office building, as shown in Fig. 8(c). The duration curve of total electric demand (Fig. 8(d)) indicates that, compared to air-cooled chiller system, the implementation of seawater cooled chiller system will reduce the peak power from 397.9 to 361.8 kW for the office building, and from 404.7 to 372.1 kW for the hotel building.

6. Results and discussions

In this section, techno-economic-environmental performances of distributed BIPVs and oscillating water column systems in a coastal community are analysed. Multi-criteria performance enhancement provided from different energy management strategies is quantified and compared. Multi-dimensional energy management strategies are included, like mobility vehicle integration, synergistic collaboration between renewable and grid systems. Afterwards, based on solar and ocean energy resources in Hong Kong, geographical location planning schemes and dynamic power dispatch strategies are studied with frontier guidelines on coastal district communities.

6.1. Potentials of distributed BIPVs and oscillating water column on the served community scale

To quantify the potentials of distributed BIPVs and oscillating water column systems on the served scale of coastal community, multi-criteria

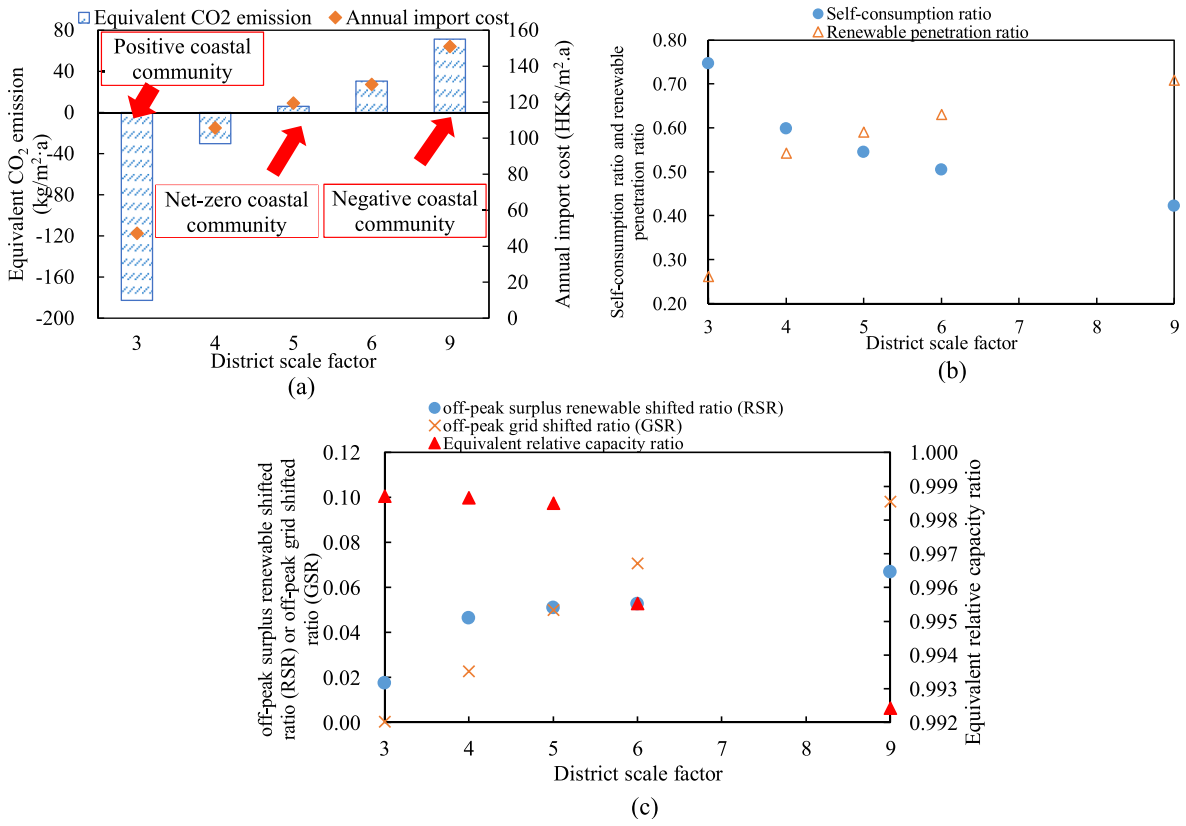

Fig. 9. Impact of district scale factor on multiple performances of the served coastal community with distributed BIPVs and oscillating water column: (a) economic and environmental performances; (b) energy matching; (c) energy flexibility and equivalent RC.
(Note: Control Strategy 1 is adopted without V2B interaction.)

performances of the coastal community are studied with different served community scales. The district scale factor is used to represent the scale of the coastal community, with the expansion on both buildings and vehicles. To be more specific, the district scale factor at 3 indicates that, there are 3 high-rise office buildings, 3 high-rise hotel buildings, and the number of vehicles is 3 times the scale as listed in Table 4.

Fig. 9 shows the evolution of multi-criteria performance of the coastal community, in respect to different district scale factors. As illustrated in Fig. 9(a), the increase of the district scale factor will lead to the energy paradigm transition from positive to negative. Specifically, the increase of the district scale factor from 3 to 9 leads to the increase of the ECE from −182.6 to 71.3 kg/m^2·a, and the annual import cost from 47.2 to 150.9 HK$/m^2·a. It can be noticed that, the hybrid renewable systems with distributed BIPVs and oscillating water column can lead to the net-zero coastal community with the district scale factor at 5. In other words, with the integrated of BIPVs and ocean energy of oscillating water column in Hong Kong, a district community can become net-zero energy, consisting of 5 high-rise office buildings, 5 high-rise hotel buildings, 150 private cars and 120 public shuttle buses.

In terms of the energy matching, with the increase of the district scale factor from 3 to 9, the self-consumption ratio decreases from 74.6% to 42.2%, whereas the renewable penetration ratio increases from 26.2% to 70.9%. The former is due to the increase of energy demands from 5.2×10^6 to 2.9×10^7 kWh/a, and the latter is due to the decrease of the grid exportation from 1.11×10^7 to 5.95×10^6 kWh/a. In other words, with the increase of the district scale factor from 3 to 9, the proportion of the energy demands being covered by renewable energy is decreased from 74.6% to 42.2%. Meanwhile, the proportion of the renewable energy consumed in the coastal energy community is increased from 26.2% to 70.9%.

Energy flexibility and RC battery, as shown in Fig. 9c indicates that, the increase of the district scale factor from 3 to 9 leads to the increase of the RSR from 0.017 to 0.067, and the GSR from 0 to 0.098. The main reason is due to the enhancement of battery storage capacity and the increase in energy demands. It is noteworthy that, the increase of the district scale factor from 3 to 9 will contribute to the decrease of the equivalent relative capacity ratio from 0.9987 to 0.9924. The main reason is due to the increase in battery storage capacity.

6.2. *Comparison on energy management and multi-criteria performance analysis*

In this section, investigation on different energy paradigms was conducted. The ultimate target is to provide robust energy management strategies for system manager with superior techno-economic performance and high energy flexibility.

As shown in Fig. 10(a), compared to isolated system, the V2B interaction will reduce the annual import cost, i.e., from 150.9 to 149.8 HK$/m^2·a by 0.8% in the negative energy community, from 119.5 to 117.2 HK$/m^2·a by 1.9% in the net-zero energy community, and from 47.2 to 44.4 HK$/m^2·a by 5.9% in the positive energy community. The reason is due to the expansion of energy system boundary in the V2B interaction scheme, leading to the increase of self-consumption ratio (from 42.6% to 46.5% in the negative energy community, from 55.3% to 58.7% in the net-zero energy community, and from 68.4% to 74.6% in the positive energy community, as shown in Fig. 10(c)) and the decrease of the imported energy from the grid. Furthermore, as shown in Fig. 10 (a), compared to Control Strategy 1 with annual import cost at 149.7 HK $/m^2·a, the grid-responsive control (Control Strategy 2) and the battery-protective control (Control Strategy 3) will increase the annual import cost to 175.6 and 175.4 HK$/m^2·a in the negative energy community, respectively. The main reason is due to the unobvious difference between peak and off-peak electric tariff in Hong Kong (only 0.2 HK $/kWh), and the increased battery charging loss due to the grid-to-

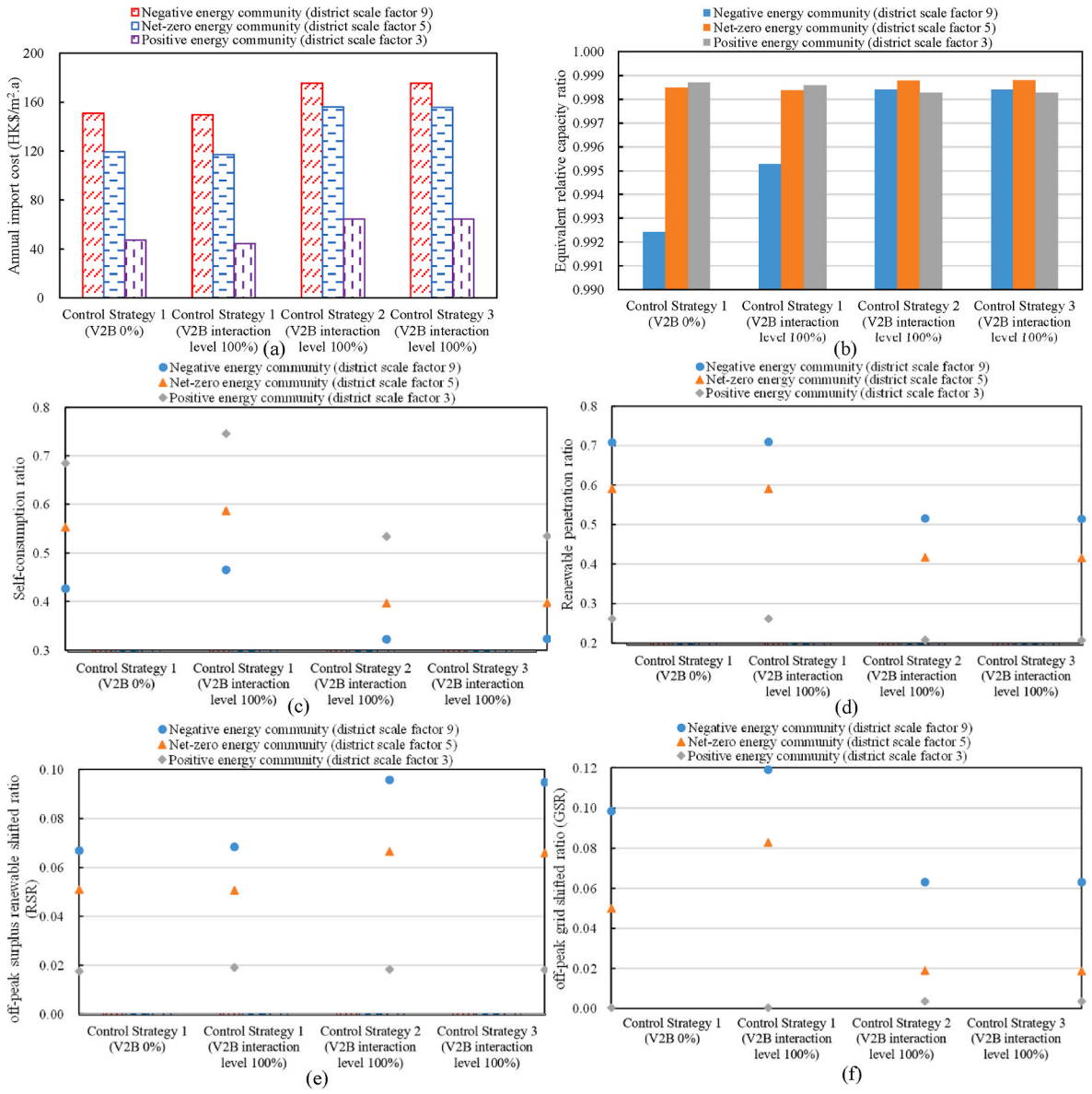

Fig. 10. Comparative analysis: (a) annual import cost; (b) equivalent relative capacity of battery; (c) self-consumption ratio; (d) renewable penetration ratiI(e) RSR; (f) GSR.

battery charging process.

In terms of $RC_{equivalent}$, as shown in Fig. 10(b), compared to the Control Strategy 1 (V2B 0%), the adoption of the Control Strategy 3 (battery-protective control) will improve the $RC_{equivalent}$. Furthermore, compared to the positive energy paradigm, the impact of Control Strategy 3 (battery-protective control) on $RC_{equivalent}$ is more obvious in the negative and net-zero energy community, e.g., from 0.9924 to 0.9984 in the negative energy community, and from 0.9985 to 0.9988 in the net-zero energy community.

The energy matching performance, as shown in Fig. 10(c), indicates that, the V2B interaction level will improve the self-consumption ratio and the renewable penetration ratio, whereas the implementation of the grid-to-battery charging strategy in the Control Strategy 2 and 3, will lead to the decrease of both self-consumption ratio and renewable penetration ratio. This is because of the energy congestion for energy shifting via the limited battery storage systems.

The energy flexibility, as shown in Fig. 10(e), indicates that, compared to the Control Strategy 1 (V2B 0%), the Control Strategy 1 (V2B interaction level at 100%) will slightly increase the RSR (from 6.68% to 6.83% in the negative energy paradigm), and the adoption of Control Strategy 2 and 3 will obviously improve the RSR to 9.57% and 9.48% in the negative energy paradigm, respectively. The former is due to the increase in battery storage capacity, and the latter is due to the increase in renewable electricity shifting. The off-peak grid shifted ratio (GSR) in Fig. 10(f), indicates that, compared to the Control Strategy 1 (V2B 0%), the Control Strategy 1 (V2B interaction level at 100%) will slightly increase the GSR (from 9.82% to 11.90% in the negative energy paradigm), and the adoption of Control Strategy 2 and 3 will contrarily decrease the GSR to 6.30% in the negative energy paradigm. The former is due to the decrease of the annual imported electricity from 1.68×10^7 to 1.57×10^7 kWh/a, and the latter is due to the increase of the annual imported electricity to $1.99 \times 10^7$and 1.98×10^7 kWh/a, respectively.

It can be summarized that, the battery-protective control (Control Strategy 3) can slow down the battery cycling aging rate and improve the equivalent relative capacity of batteries, whereas the system import cost is increased due to the high off-peak grid tariff and the increased battery charging losses. Furthermore, due to the energy congestion with renewable energy, the Control Strategy 3 will result in low self-

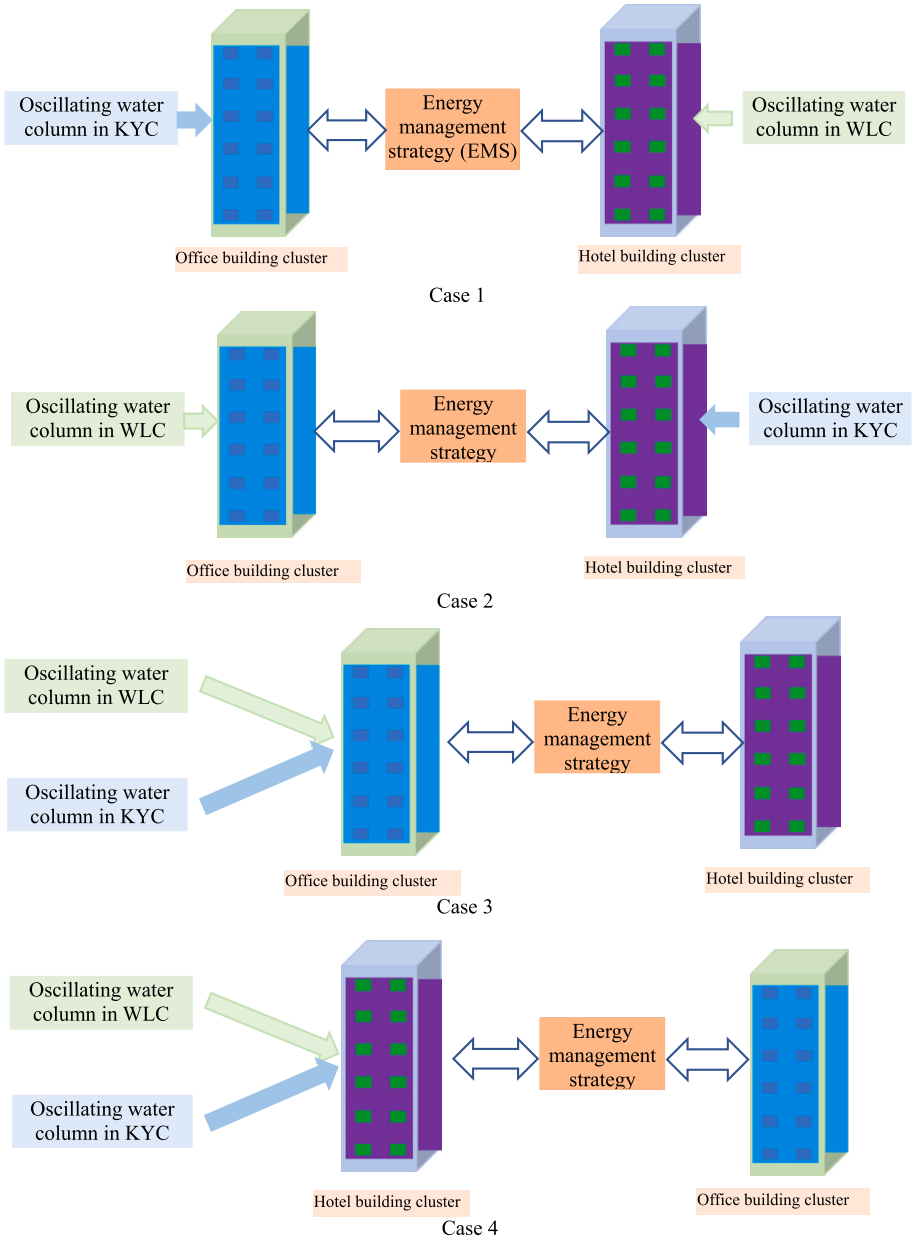

Fig. 11. Geographical location planning schemes for coastal community buildings.

consumption ratio and low renewable penetration ratio.

6.3. Geographical location of office and hotel buildings

6.3.1. Energy system planning and structural configurations

Fig. 11 shows the structural configuration and geographical location planning schemes for coastal community buildings. As shown in Fig. 11, two types of renewable systems are designed, i.e., oscillating water column and distributed BIPVs. Energy demands of both buildings and transportations are considered. As shown in Fig. 11, depending on the geographical location and planning of district building community, different geographical location planning schemes have been proposed. The ultimate target is to provide planning schemes on coastal community buildings, with enhanced techno-economic performances.

Table 5 summarizes geographical location planning of coastal community buildings. The differences between different geographical location planning schemes can be summarized as follows:

1) In Case 1 and 2, renewable energies from solar-based BIPVs and oscillating water column are firstly managed to cover the energy demand of associated buildings, and then to be shared by other buildings through the V2B integrations and the mobile battery storage of vehicles.
2) In the Case 3, both solar-based BIPVs and oscillating water column are designed for office buildings, whereas only BIPVs are for hotel buildings. Surplus energy can be shared between different types of buildings, through the V2B integrations and the mobile battery storage of vehicles.
3) In the Case 4, both solar-based BIPVs and oscillating water column are designed for hotel buildings, whereas only BIPVs are for office buildings. Surplus energy can be shared between different types of buildings, through the V2B integrations and the mobile battery storage of vehicles.

6.3.2. Multi-criteria performance comparison

Fig. 12 shows the techno-economic performances for different

Table 5
Summary of the geographical location planning for coastal community buildings.

Cases	Geographical location of buildings	Remarks
Case 1	Office buildings close to KYC, and hotel buildings close to WLC	Renewable energies from solar-based BIPVs and oscillating water column are firstly managed to cover the energy demand of associated buildings, and then to be shared by other buildings. The difference between Case 1 and 2 is the geographical location of each building.
Case 2	Office buildings close to WLC, and hotel buildings close to KYC	
Case 3	Only office buildings are planned close to all power supply with oscillating water column	Both solar-based BIPVs and oscillating water column are designed for office buildings, whereas only BIPVs are for hotel buildings.
Case 4	Only hotel buildings are planned close to all power supply with oscillating water column	Both solar-based BIPVs and oscillating water column are designed for hotel buildings, whereas only BIPVs are for office buildings.

geographical location planning schemes on coastal community buildings. As shown in Fig. 12(a), the Case 1 shows the lowest annual import cost at 117.2 HK$/m^2·a, which is 20.2% lower than that of the Case 3 at 146.8 HK$/m^2·a. Meanwhile, the Case 1 also shows the lowest ECE at 3.9 kg/m^2·a, which is 59.2% lower than that of the Case 3 at 9.6 kg/m^2·a. The underlying mechanism can be summarized as follows: as shown in Fig. 12(b), the Case 1 shows the highest self-consumption ratio at 58.7%, leading to the lowest import energy from the power grid and the lowest annual import cost. Meanwhile, the Case 1 shows the highest renewable penetration ratio at 59.0%, leading to the lowest battery charging losses and the lowest ECE. Regarding energy flexibility for power shifting in Fig. 12(c), compared to other cases, the Case 1 shows the highest RSR at 5.1%, whereas the Case 3 shows the lowest RSR at 1.2%. Meanwhile, the Case 3 shows the highest GSR at 12%. Regarding equivalent relative capacity of batteries in Fig. 12(d), different cycling aging magnitudes can be noticed, depending on the geographical location planning schemes. Among all formulated cases, the Case 3 shows the lowest battery cycling aging with the highest $RC_{equivalent}$ at 0.9988, whereas the Case 2 shows the highest battery cycling aging with the lowest $RC_{equivalent}$ at 0.9965.

In summary, the geographical location planning scheme on the Case 1 (office buildings close to KYC, and hotel buildings close to WLC) is the most economically and environmentally feasible scheme, whereas the Case 3 (only office buildings are planned close to all power supply with oscillating water column) shows the highest flexibility in grid electricity shifting, together with the highest $RC_{equivalent}$.

6.4. *Research limitations, challenges and future perspectives*

This study provides geographical location plans and energy management strategies on frontier ocean thermal/power and solar PV systems for transformation towards net-zero coastal communities. In addition to coastal communities, research results have widespread and promising application potentials in other regions. Firstly, the developed model can help plan, design and optimize multi-energy systems in communities for energy-efficient and sustainability transitions.

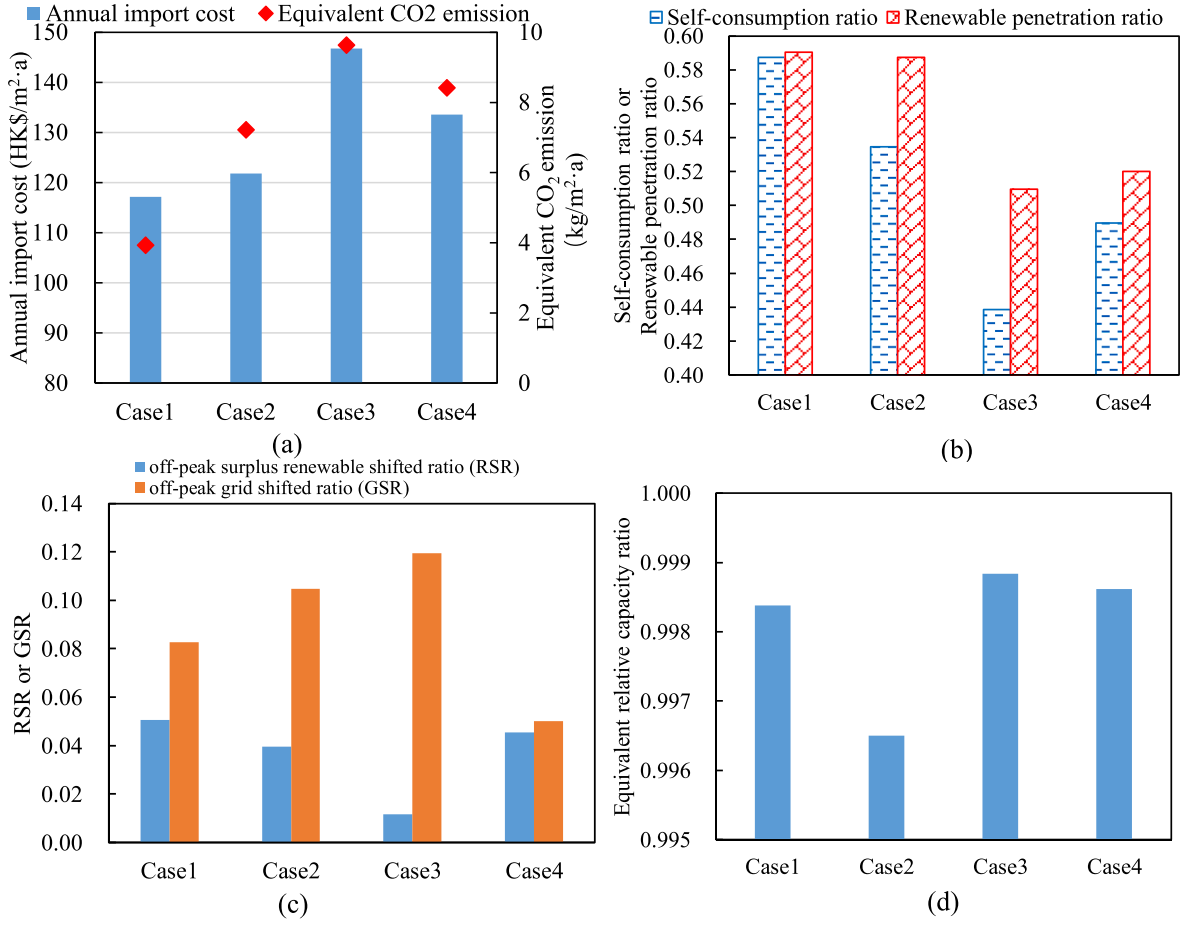

Fig. 12. Impact of different geographical locations of coastal buildings on multi-criteria performances: (a) economic and environmental performances; (b) energy matching; (c) energy flexibility; (d) equivalent relative capacity of batteries.

Secondly, availability and techno-economic feasibility of time-of-use prices in local power grid can be analysed throughout the demand-side response, thermal/electric energy storages, and even grid-response strategies. However, there are some research limitations need to be clarified. Firstly, in terms of wave energy data (like wave height, wave period and wavelength), only two locations within average data for three years (2017, 2018 and 2019) are used without in-depth analysis on the evolution of wave resource data. Secondly, mathematical models on oscillating water columns are with ideal assumptions without considering the decrease in power generation due to mechanical degradation. Thirdly, indoor occupancy models and integrated vehicle driving models are full of stochastic characteristics without onsite data calibration. Based on these assumptions, future studies will focus on wave power analysis based on historical wave energy data over last several decades to obtain a more comprehensive understanding of wave resources. Afterwards, mathematical models on oscillating water column and occupancy models will be validated and calibrated by experimental data to improve these models to reflect real-world conditions.

7. Conclusions

In this study, an integrated platform was developed for energy planning, design, operation of a coastal district community. The impact analysis of energy synergies on techno-economic-environmental performance was conducted, in respect to centralised seawater-based chiller systems, distributed BIPVs and coastal oscillating water columns, and smart Vehicle-to-Building interactions. Energy management strategies were implemented and contrasted to enhance renewable penetration, reduce import cost and decelerate battery cycling aging, in response to relative renewable-to-demand difference, off-peak grid information with low price, and real-time battery cycling aging. In accordance with the statistical data of two wave stations (i.e., Kau Yi Chau (KYC) and West Lamma Channel (WLC)) in Hong Kong, energy system planning and structural configurations of the coastal community have been proposed. Research results are summarized as follows:

1) compared to an air-cooled chiller system, the water-cooled chiller will reduce the energy consumption of AHU cooling system from 6.9 to 3.8 kWh/m^2·a, the space cooling system from 11.3 to 6.9 kWh/m^2·a, and total electric demand from 134 to 126.5 kWh/m^2·a.
2) based on local solar and ocean energy resources, the scale for the net-zero coastal community with distributed BIPVs and oscillating water column was identified as 5 high-rise office buildings, 5 high-rise hotel buildings, 150 private cars and 120 public shuttle buses. In the net-zero coastal community, the annual import cost is 119.5 HK $/$m^2$·a, with 54.4% of energy demand being covered by renewable energy and 59% of renewable energy being consumed in the coastal community.
3) energy system design, planning and operation indicate that, dynamic grid price is required for cost-savings. In order to overcome the battery depreciation cost and battery charging loss, the increase in price difference between peak and off-peak periods is an effective solution, so as to attract more vehicle owners to participate in the energy sharing paradigm.
4) the geographical location planning scheme on Case 1 (office buildings close to KYC, and hotel buildings close to WLC) is the most economically and environmentally feasible scheme, with the lowest annual import cost at 117.2 HK$/$m^2$·a and the lowest equivalent CO_2 emission at 3.9 kg/m^2·a. Meanwhile, Case 3 (only office buildings are planned close to all power supply with oscillating water column) shows the highest flexibility for shifting the off-peak grid electricity to peak period (grid shifted ratio at 12%), together with the highest value of equivalent battery relative capacity ($RC_{equivalent}$ at 0.9988).

Future studies will focus on stochastic optimisation of both building occupants' behaviours and EV driving schedules. Furthermore, economic performance of different stakeholders will be studied with incentives to promote multi-stakeholders' proactivity and market vitality. The multi-objective optimisation and decision-making will be conducted to identify the 'best-of-the-best' solution for zero-carbon and sustainability transitions.

Credit author statement

Zhengxuan Liu: Data curation; Formal analysis; Investigation; Methodology; Software; Roles/Writing - original draft; Writing - review & editing. Yuekuan Zhou: Conceptualization; Data curation; Formal analysis; Investigation; Methodology; Resources; Software; Supervision; Roles/Writing - original draft; Writing - review & editing. Jun Yan: Data curation; Formal analysis; Investigation; Methodology; Roles/Writing - original draft; Writing - review & editing. Marcos Tostado-Véliz: Investigation; Methodology; Writing - review & editing.

Declaration of competing interest

The authors declare that they have no known competing financial interests or personal relationships that could have appeared to influence the work reported in this paper.

Data availability

The data that has been used is confidential.

Acknowledgements

This work was supported by Regional joint fund youth fund project (2022A1515110364, P00038-1002), Basic and Applied Basic Research Project-Guangzhou 2023 (2023A04J1035, P00121-1003), Joint Funding of Institutes and Enterprises in 2023 (2023A03J0104) and HKUST (GZ)-enterprise cooperation project (R00017-2001). This research is supported by The Hong Kong University of Science and Technology (Guangzhou) startup grant (G0101000059). This work was also supported in part by the Project of Hetao Shenzhen-Hong Kong Science and Technology Innovation Cooperation Zone (HZQB-KCZYB-2020083).

References

[1] Liu Z, Sun Y, Xing C, Liu J, He Y, Zhou Y, et al. Artificial intelligence powered large-scale renewable integrations in multi-energy systems for carbon neutrality transition: challenges and future perspectives. Energy AI 2022;10:100195. https://doi.org/10.1016/j.egyai.2022.100195.
[2] Zhou Y, Zheng S, Liu Z, Wen T, Ding Z, Yan J, et al. Passive and active phase change materials integrated building energy systems with advanced machine-learning based climate-adaptive designs, intelligent operations, uncertainty-based analysis and optimisations: a state-of-the-art review. Renew Sustain Energy Rev 2020;130:109889. https://doi.org/10.1016/j.rser.2020.109889.
[3] He Y, Zhou Y, Liu J, Liu Z, Zhang G. An inter-city energy migration framework for regional energy balance through daily commuting fuel-cell vehicles. Appl Energy 2022;324:119714. https://doi.org/10.1016/j.apenergy.2022.119714.
[4] Zhou Y. Transition towards carbon-neutral districts based on storage techniques and spatiotemporal energy sharing with electrification and hydrogenation. Renew Sustain Energy Rev 2022;162:112444. https://doi.org/10.1016/j.rser.2022.112444.
[5] Zhou Y. Energy sharing and trading on a novel spatiotemporal energy network in Guangdong-Hong Kong-Macao Greater Bay Area. Appl Energy 2022;318:119131. https://doi.org/10.1016/j.apenergy.2022.119131.
[6] Luo S, Hu W, Liu W, Zhang Z, Bai C, Huang Q, et al. Study on the decarbonization in China's power sector under the background of carbon neutrality by 2060. Renew Sustain Energy Rev 2022;166:112618. https://doi.org/10.1016/j.rser.2022.112618.
[7] Zhou Y, Liu Z. A cross-scale 'material-component-system' framework for transition towards zero-carbon buildings and districts with low, medium and high-temperature phase change materials. Sustain Cities Soc 2023;89:104378. https://doi.org/10.1016/j.scs.2022.104378.
[8] You K, Yu Y, Cai W, Liu Z. The change in temporal trend and spatial distribution of CO2 emissions of China's public and commercial buildings. Build Environ 2023;229:109956. https://doi.org/10.1016/j.buildenv.2022.109956.

[9] Zhou Y. Ocean energy applications for coastal communities with artificial intelligencea state-of-the-art review. Energy AI 2022;10:100189. https://doi.org/10.1016/j.egyai.2022.100189.
[10] Hu H, Xue W, Jiang P, Li Y. Bibliometric analysis for ocean renewable energy: an comprehensive review for hotspots, frontiers, and emerging trends. Renew Sustain Energy Rev 2022;167:112739. https://doi.org/10.1016/j.rser.2022.112739.
[11] Qiu S, Liu K, Wang D, Ye J, Liang F. A comprehensive review of ocean wave energy research and development in China. Renew Sustain Energy Rev 2019;113:109271. https://doi.org/10.1016/j.rser.2019.109271.
[12] Melikoglu M. Current status and future of ocean energy sources: a global review. Ocean Eng 2018;148:563–73. https://doi.org/10.1016/j.oceaneng.2017.11.045.
[13] Rehman S, Alhems LM, Alam MdM, Wang L, Toor Z. A review of energy extraction from wind and ocean: technologies, merits, efficiencies, and cost. Ocean Eng 2023;267:113192. https://doi.org/10.1016/j.oceaneng.2022.113192.
[14] Song Y, Akashi Y, Yee J-J. Effects of utilizing seawater as a cooling source system in a commercial complex. Energy Build 2007;39:1080–7. https://doi.org/10.1016/j.enbuild.2006.11.011.
[15] Li M, Luo H, Zhou S, Senthil Kumar GM, Guo X, Law TC, et al. State-of-the-art review of the flexibility and feasibility of emerging offshore and coastal ocean energy technologies in East and Southeast Asia. Renew Sustain Energy Rev 2022;162:112404. https://doi.org/10.1016/j.rser.2022.112404.
[16] Viviano A, Naty S, Foti E, Bruce T, Allsop W, Vicinanza D. Large-scale experiments on the behaviour of a generalised Oscillating Water Column under random waves. Renew Energy 2016;99:875–87. https://doi.org/10.1016/j.renene.2016.07.067.
[17] Elhanafi A, Fleming A, Macfarlane G, Leong Z. Numerical energy balance analysis for an onshore oscillating water column–wave energy converter. Energy 2016;116:539–57. https://doi.org/10.1016/j.energy.2016.09.118.
[18] Falcão AFO, Henriques JCC. Oscillating-water-column wave energy converters and air turbines: a review. Renew Energy 2016;85:1391–424. https://doi.org/10.1016/j.renene.2015.07.086.
[19] Icaza-Alvarez D, Jurado F, Tostado-Véliz M. Long-term planning for the integration of electric mobility with 100% renewable energy generation under various degrees of decentralization: case study Cuenca, Ecuador. Energy Rep 2023;9:4816–29. https://doi.org/10.1016/j.egyr.2023.03.118.
[20] Erdinc O, Uzunoglu M. Optimum design of hybrid renewable energy systems: overview of different approaches. Renew Sustain Energy Rev 2012;16:1412–25. https://doi.org/10.1016/j.rser.2011.11.011.
[21] Upadhyay S, Sharma MP. A review on configurations, control and sizing methodologies of hybrid energy systems. Renew Sustain Energy Rev 2014;38:47–63. https://doi.org/10.1016/j.rser.2014.05.057.
[22] Liu Y, Yu S, Zhu Y, Wang D, Liu J. Modeling, planning, application and management of energy systems for isolated areas: a review. Renew Sustain Energy Rev 2018;82:460–70. https://doi.org/10.1016/j.rser.2017.09.063.
[23] Zhou Z, Benbouzid M, Frédéric Charpentier J, Scuiller F, Tang T. A review of energy storage technologies for marine current energy systems. Renew Sustain Energy Rev 2013;18:390–400. https://doi.org/10.1016/j.rser.2012.10.006.
[24] Zhou Y, Cao S, Hensen JLM, Hasan A. Heuristic battery-protective strategy for energy management of an interactive renewables–buildings–vehicles energy sharing network with high energy flexibility. Energy Convers Manag 2020;214:112891. https://doi.org/10.1016/j.enconman.2020.112891.
[25] Zhou Y, Cao S. Coordinated multi-criteria framework for cycling aging-based battery storage management strategies for positive building–vehicle system with renewable depreciation: life-cycle based techno-economic feasibility study. Energy Convers Manag 2020;226:113473. https://doi.org/10.1016/j.enconman.2020.113473.
[26] Icaza-Alvarez D, Arias Reyes P, Jurado F, Tostado-Véliz M. Smart strategies for the penetration of 100% renewable energy for the Ecuadorian Amazon region by 2050. J Clean Prod 2023;382:135298. https://doi.org/10.1016/j.jclepro.2022.135298.
[27] Zhou Y, Cao S. Energy flexibility investigation of advanced grid-responsive energy control strategies with the static battery and electric vehicles: a case study of a high-rise office building in Hong Kong. Energy Convers Manag 2019;199:111888. https://doi.org/10.1016/j.enconman.2019.111888.
[28] Pascual J, Barricarte J, Sanchis P, Marroyo L. Energy management strategy for a renewable-based residential microgrid with generation and demand forecasting. Appl Energy 2015;158:12–25. https://doi.org/10.1016/j.apenergy.2015.08.040.
[29] Croce D, Giuliano F, Bonomolo M, Leone G, Musca R, Tinnirello I. A decentralized load control architecture for smart energy consumption in small islands. Sustain Cities Soc 2020;53:101902. https://doi.org/10.1016/j.scs.2019.101902.
[30] Meng Q, Xiong C, Mourshed M, Wu M, Ren X, Wang W, et al. Change-point multivariable quantile regression to explore effect of weather variables on building energy consumption and estimate base temperature range. Sustain Cities Soc 2020;53:101900. https://doi.org/10.1016/j.scs.2019.101900.
[31] de Rubeis T, Falasca S, Curci G, Paoletti D, Ambrosini D. Sensitivity of heating performance of an energy self-sufficient building to climate zone, climate change and HVAC system solutions. Sustain Cities Soc 2020;61:102300. https://doi.org/10.1016/j.scs.2020.102300.
[32] Zhou Y, Cao S. Quantification of energy flexibility of residential net-zero-energy buildings involved with dynamic operations of hybrid energy storages and diversified energy conversion strategies. Sustain Energy Grids Netw 2020;21:100304. https://doi.org/10.1016/j.segan.2020.100304.
[33] Yan J, Menghwar M, Asghar E, Kumar Panjwani M, Liu Y. Real-time energy management for a smart-community microgrid with battery swapping and renewables. Appl Energy 2019;238:180–94. https://doi.org/10.1016/j.apenergy.2018.12.078.
[34] Zhou Y, Cao S, Hensen JLM. An energy paradigm transition framework from negative towards positive district energy sharing networks—battery cycling aging, advanced battery management strategies, flexible vehicles-to-buildings interactions, uncertainty and sensitivity analysis. Appl Energy 2021;288:116606. https://doi.org/10.1016/j.apenergy.2021.116606.
[35] Liu J, Zhou Y, Yang H, Wu H. Net-zero energy management and optimization of commercial building sectors with hybrid renewable energy systems integrated with energy storage of pumped hydro and hydrogen taxis. Appl Energy 2022;321:119312. https://doi.org/10.1016/j.apenergy.2022.119312.
[36] Gao Z, Lin Z, LaClair TJ, Liu C, Li J-M, Birky AK, et al. Battery capacity and recharging needs for electric buses in city transit service. Energy 2017;122:588–600. https://doi.org/10.1016/j.energy.2017.01.101.
[37] Jordan DC, Kurtz SR. Photovoltaic degradation rates—an analytical review. Prog Photovoltaics Res Appl 2013;21:12–29. https://doi.org/10.1002/pip.1182.
[38] Sameti M, Farahi Elham. Output power for an oscillating water column wave energy conversion device. Ocean Environ Fluid Res OEFR 2014;1(a).